Available online at www.sciencedirect.com

SciVerse ScienceDirect

Solar Energy 85 (2011) 2771–2780

SOLAR ENERGY

www.elsevier.com/locate/solener

A fast and low cost analog maximum power point tracking method for low power photovoltaic systems

Yi-Hua Liu *, Jia-Wei Huang

Department of Electrical Engineering, National Taiwan University of Science and Technology, No. 43, Sec. 4, Keelung Road, Taipei 106, Taiwan, ROC

Received 9 June 2011; received in revised form 28 July 2011; accepted 15 August 2011
Available online 13 September 2011

Communicated by: Associate Editor Nicola Romeo

Abstract

Low power photovoltaic (PV) systems are commonly used in stand-alone applications. For these systems, a simple and cost-effective maximum power point tracking (MPPT) solution is essential. In this paper, a fast and low cost analog MPPT method for low power PV systems is proposed. By using two voltage approximation lines (VALs) to approximate the maximum power point (MPP) locus, a low-complexity analog MPPT circuit can be developed. Theoretical derivation and detailed design procedure will be provided in this paper. The proposed method boasts the advantages such as simple structure, low cost, fast tracking speed and high tracking efficiency. To validate the correctness of the proposed method, simulation and experimental results of an 87 W PV system will also be provided to demonstrate the effectiveness of the proposed technique.
© 2011 Elsevier Ltd. All rights reserved.

Keywords: Photovoltaic (PV); Maximum power point tracking (MPPT); Analog MPPT

1. Introduction

Researches on renewable energies have received much attention due to their capability of reducing the fossil fuels usage and mitigating the environmental issues such as the green house effect and air pollution. Among them, the photovoltaic (PV) generation system has become increasingly important as a renewable source due to its advantages such as absence of fuel cost, low maintenance requirement and environmental friendliness. There exist two main problems when operating a PV generation system – the conversion efficiency is very low, especially under low irradiation, and the amount of the electric power generated by solar cells varies with weather conditions, i.e., the solar insolation and panel temperature. To overcome these problem, a maximum power point tracking (MPPT) method, which has quick response and is able to make good use of the electric power generated in both high and low irradiation levels, is required (Dasgupta et al., 2008; Chu and Chen, 2009; Wang et al., 2011; Messai et al., 2011; Kakosimos and Kladas, 2011). Many MPPT methods have been developed and implemented. These methods vary in complexity, sensors required, convergence speed, cost and range of effectiveness (Hohm and Ropp, 2003; Salas et al., 2006; Esram and Chapman, 2007). Typically, MPPT methods utilized in medium and high power PV systems uses measured cell characteristics (current, voltage, power) along with an online search algorithm to compute the corresponding maximum power point (MPP). Due to the complexity of the required mathematical operations, a digital signal processor (DSP) or a relatively powerful microcontroller (μC) is typically needed, which increases the cost of the system. However, in low power PV systems (from a few watts up to a few hundreds of watt) which are frequently used as stand-alone power supplies for mobile applications, remote measurement and communication systems, LED lighting systems, and road

* Corresponding author. Tel.: +886 27301252; fax: +886 27376699.
E-mail addresses: yhliu@mail.ntust.edu.tw (Y.-H. Liu), D9707203@mail.ntust.edu.tw (J.-W. Huang).

0038-092X/$ - see front matter © 2011 Elsevier Ltd. All rights reserved.
doi:10.1016/j.solener.2011.08.019

traffic signs, μCs or DSPs and the related analog conditioning circuit may not be cost-effective. Moreover, it consumes significant portion be cost-effective. Moreover, it consumes significant portion of the generated power. Therefore, an analog MPPT circuit with low-cost and fast-tracking features is essential.

Various analog MPPT techniques have been proposed in the literatures. The fractional open circuit voltage method exploits the nearly linear relationship between the PV panel open circuit voltage (OCV) and its voltage at the MPP. This strategy is very simple. However, periodical disconnection of the PV panel for OCV measurement results in a temporary loss of power (Ahmad, 2010). An alternative is to use one pilot cell which has the same characteristics as the panels in the array. This method is unsuitable for low power applications where cost and size are important designing constraints (Dondi et al., 2008). Analog versions of the widely-adopted Perturb and Observe (P&O) based methods have been presented in the literatures (Leyva et al., 2006; Enrique et al., 2010; Lopez-Lapena et al., 2010). The basic idea of P&Q method is to slightly perturb the operating voltage of the PV panel and see how the power changes. If the power increases, the perturbation should be kept in the same direction; otherwise, it should be reversed. The analog P&O method is accurate, fast and reliable. However, the implementation of the analog version of P&O often requires analog multiplier, which makes the system complex and uneconomical. Analog versions of another popular incremental conductance technique (ICT) can be found in Chung et al. (2003) and Mattavelli et al. (2010). In Chung et al. (2003), the input resistance and the voltage stress are used to locate the MPP. These relationships are derived from a SEPIC (or Cuk) converter under discontinuous capacitor voltage mode. Thus, the application of this technique is limited. On the other hand, the MPPT circuit presented in Mattavelli et al. (2010) contains both analog and digital part, which complicates the design. The ripple correlation control (RCC) method has been proved to be a suitable technique for analog implementation (Esram et al., 2006). RCC correlates the time derivative of power with the time derivative of current or voltage to drive the power gradient to zero and reach the MPP. RCC yields fast and parameter-insensitive MPPT of PV systems. However, the inductive and capacitive parasitic components may have a significant impact on the ability of RCC to drive the system toward the true MPP. Moreover, analog multiplier is also necessary. A specially designed MPPT IC is proposed in Hsieh et al. (2010), the presented IC is fast and accurate, but dedicated hardware is required. Multi-module-based MPPT approaches have been presented in Park et al. (2006) and Femia et al. (2003); these methods measure and compare the output of two or more modules to track the MPP. These approaches are simple because no multiplication for power calculation is required. However, these methods require two or more solar arrays with similar $V-I$ characteristics; therefore are more suitable for distributed PV generation systems. A less complicated way of tracking the MPP is through an estimation technique, based on an offline module characterization. The linear relationship between the values of panel voltage and current at the MPP can be used to accelerate the speed of the MPPT algorithm. The devised method not only can track the MPP instantaneously but also can be implemented easily (Pan et al., 1999; Sokolov and Shmilovitz, 2008; Scarpa et al., 2009). However, these methods present poor tracking efficiencies for low irradiation levels. There are also some MPPT products for low power PV systems available in the market recently (Texas Instrument, 2009; National Semiconductor, 2011; STMicroelectronics, 2011). For the product presented in Texas Instrument (2009), constant voltage method is utilized so the tracking efficiency is lower. For those products provided by National Semiconductor (2011) and STMicroelectronics (2011), digital P&O core is required, which complicates the design. In addition, digital P&O has slower response time comparing to their analog counterparts.

In this paper, a fast and low complexity analog MPPT method that is particularly suitable for low power PV systems is proposed. The presented technique models the nonlinear V–I characteristics of the solar panel using numerical approximations similar to that presented in Scarpa et al. (2009). To improve the tracking efficiency, an additional approximation line is employed to model MPP locus under low solar insolation conditions. The proposed approach is simple because it performs MPPT not only without sophisticated digital sampling and the multiplication for power calculation but also without memory storages. As a result, the proposed method can be implemented with low-cost, low-power analog components. The analog circuit implementation principle boasts the advantages of cost competitiveness and compactness of the size. The analog loop also provides a fast response to sudden changes of irradiance levels which helps to improve the PV system efficiency (Petreuş et al., 2011). In addition, the proposed method can easily be integrated into commercially available charger or pulse-width modulated (PWM) IC to aid in tracking the solar panel's MPP, which makes single-chip IC implementation possible (Texas Instruments Corp., 2011). Since the proposed method utilizes prior examination of the solar panel characteristics, the effect of panel temperature should also be considered. Hence, the proposed method suggests a simple and effective way to compensate temperature variation effect. By using a negative temperature coefficient (NTC) thermistor, a low-cost solution can be developed that allows the MPP to be tracked over various temperatures. Finally, simulation and experimental results will be provided to validate the effectiveness of the proposed method.

2. Theoretical background

For PV panels, the MPP locus can be defined as the point (V_{MP}, I_{MP}), which is a function of panel irradiation at a given operating temperature. According to Scarpa et al. (2009), the MPP locus can be approximates by a

linear equation. In this section, the analytical derivation of the MPP locus will be provided.

Fig. 1 shows the equivalent circuit of the PV cell. The basic equation from the theory of semiconductors that mathematically describes the V–I characteristic of the PV cell is

$$I_{pv} = I_g - I_S\left(\exp\left(\frac{q(V_{pv}+I_{pv}\cdot R_S)}{nkT}\right)-1\right) - \frac{V_{pv}+I_{pv}\cdot R_S}{R_P} \quad (1)$$

where n is the ideality factor, k is the Boltzmann's constant, q is the electron charge, T is the temperature in Kelvin, R_S is the equivalent series resistance, R_P is the equivalent shunt resistance and I_g, I_{pv} and I_s are the photogenerated current, panel current and saturation currents, respectively.

Generally speaking, the cell shunt resistance R_P is relatively high, thus the current through it can be neglected. Consequently, Eq. (1) becomes

$$I_{pv} = I_g - I_S\left(\exp\left(\frac{q(V_{pv}+I_{pv}\cdot R_S)}{nkT}\right)-1\right) \quad (2)$$

The panel output power can then be calculated as

$$P_{pv} = V_{pv}\cdot\left[I_g - I_S\left(\exp\left(\frac{q(V_{pv}+I_{pv}\cdot R_S)}{nkT}\right)-1\right)\right] \quad (3)$$

Base on the fact that the MPP occurs at the knee of the curve where $\partial P_P/\partial V_{PV} = 0$, the relationship between the maximum power voltage V_{MP} and the maximum power current I_{MP} can be expressed as

$$\ln\left(1+\frac{I_g}{I_S}\right) = \frac{q(V_{mp}+I_{mp}\cdot R_S)}{nkT} + \ln\left(1+\frac{qV_{mp}}{nkT}\right) \quad (4)$$

To simplify Eq. (4), the open circuit voltage V_{OC} can be obtained from Eq. (2) by setting the panel current $I_{PV} = 0$.

$$\ln\left(1+\frac{I_g}{I_S}\right) = \frac{qV_{oc}}{nkT} \quad (5)$$

Combining Eqs. (4)–(6) can be derived

$$V_{OC} - V_{mp} = I_{mp}\cdot R_S + V_{OV} \quad (6)$$

In Eq. (6), the term $V_{OV} = (nkT/q)\cdot\ln(1+qV_{mp}/nkT)$ According to Scarpa et al. (2009), V_{OV}'s variations with irradiation can be neglected.

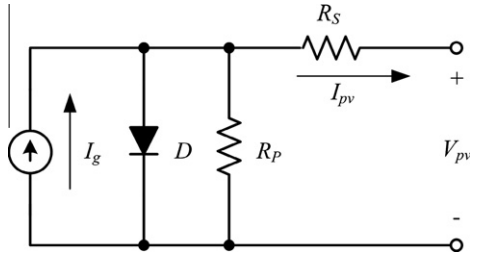

Fig. 1. Equivalent circuit of the PV cell.

Since V_{OC} is a logarithmic function of I_g, the relationship between V_{MP} and I_{MP} with respect to irradiation is not linear. However, it is possible to linearize this relationship for an interval where the value of V_{OC} is sufficiently insensitive to irradiation. That is, the voltage approximation line (VAL) can be calculated as the tangent line of the MPP locus where the sensitivity of V_{OC} to I_g ($S_{Voc,Ig}$) is lower than a pre-defined threshold. This relationship is illustrated in Fig. 2.

$$V_{mp} = \left(\left.\frac{dV_{oc}}{dI_{mp}}\right|_{I_g=I_g^*} - R_S\right)I_{mp} + V_{OFFSET} \quad (7)$$

where

$$S_{V_{OC},I_g} \equiv \frac{dV_{OC}}{V_{OC}}\cdot\frac{I_g}{dI_g} \approx \frac{1}{\ln\left(\frac{I_g}{I_{sat}}+1\right)} < S_{threshold} \quad (8)$$

From Eq. (8), the sensitivity $S_{Voc,Ig}$ is inverse proportional to the irradiation level. As a result, Eq. (7) can better approximate the MPP locus when irradiation level is high. Also from Scarpa et al. (2009), the value $dV_{OC}\sqrt{dI_{MP}}$ can be approximated by

$$\left.\frac{dV_{oc}}{dI_{mp}}\right|_{I_g=I_g^*} \approx \frac{nkT}{qI_{mp}^*} \quad (9)$$

where I_{MP}^* is the maximum power current I_{MP} obtained when $I_g = I_g^*$. So, Eq. (7) can further be simplified as

$$V_{mp} = \left(\frac{nkT}{qI_{mp}^*} - R_S\right)I_{mp} + V_{OFFSET} = kI_{MP} + V_{OFFSET} \quad (10)$$

The offset V_{OFFSET} in Eq. (10) can then be calculated by observing Fig. 2.

$$V_{OFFSET} = V_{OC}^* - V_{OV}^* - I_{mp}^*\cdot\frac{nkT}{q} \quad (11)$$

Similarly, V_{OC}^* and V_{OV}^* is V_{OC} and V_{OV} obtained when $I_g = I_g^*$, respectively. Based on the previous analysis, it is possible to implement a MPPT method by forcing the PV panel to operate over the VAL.

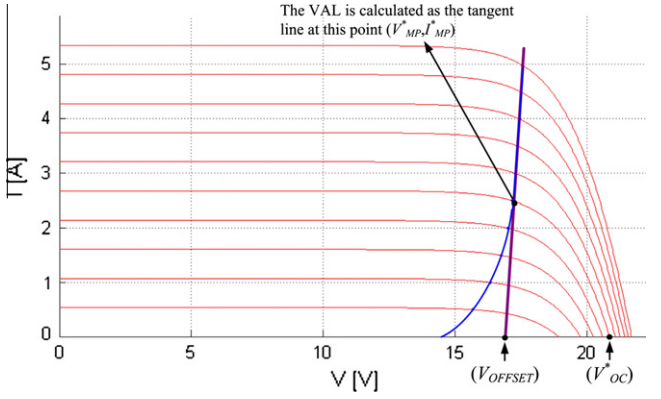

Fig. 2. I–V curves of the solar panel under different irradiation levels and the voltage approximation line.

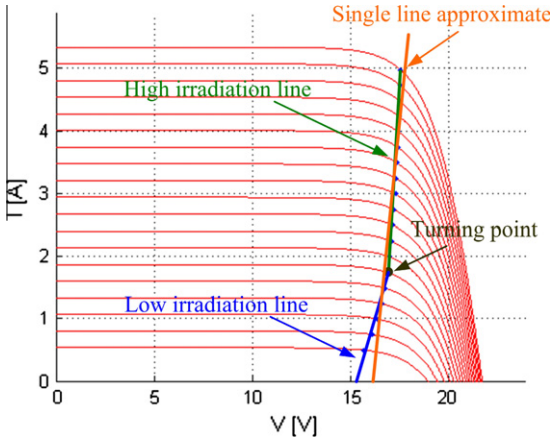

Fig. 3. *I–V* curves of the utilized solar panel under different irradiation levels.

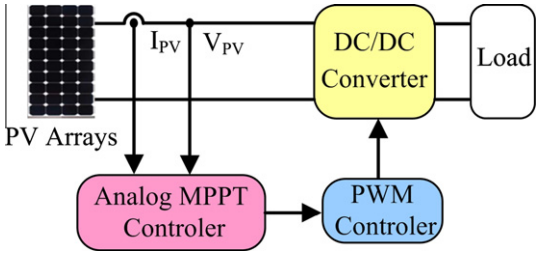

Fig. 4. The block diagram of the proposed system.

3. System configuration

From Section 2, the values of panel voltage and current at the MPP exhibit a linear relationship. Using this fact, a novel fast, low-complexity MPPT technique can be devised. In this section, the implementation method of the proposed technique will be provided in detail. To simplify the design procedure, numerical method in stead of analytical derivation is employed to obtain the approximation lines of the MPP locus in this paper. Fig. 3 shows the *I–V* curves under different irradiation levels of the utilized KC85T solar panel from Kyocera Inc. (Kyocera Inc., 2007). These curves are obtained using MATLAB simulation. The circular markers in the graphs represent the calculated MPP points (V_{MP}, I_{MP}). From Fig. 3, the MPP locus can be better modeled as two linear sections than one straight line. That is, the slope k and the offset point V_{OFFSET} should be different for high and low irradiation conditions. In summary, if the *I–V* characteristics for any PV panel can be obtained, the parameter sets (k_{HIGH}, k_{LOW}, $V_{OEESET,H}$ and $V_{OFFSET,L}$) approximating the MPP locus can be calculated using the polynomial curve fitting function *polyfit* provided by MATLAB accordingly. Using this concept, Eq. (10) can be rewritten as

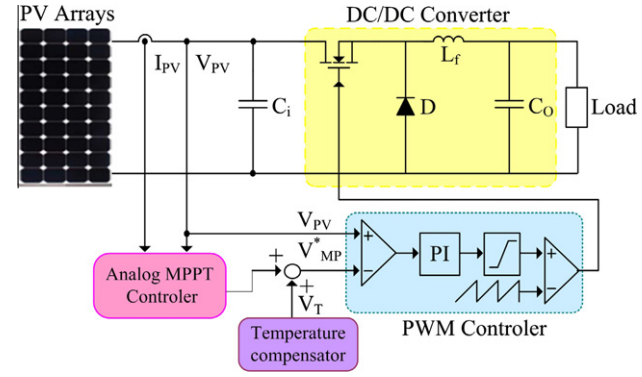

Fig. 6. Detailed implementation of the proposed method.

$$\begin{cases} V_{PV} = k_{HIGH} I_{PV} + V_{OFFSET,H}, & \text{high irradiation level} \\ V_{PV} = k_{LOW} I_{PV} + V_{OFFSET,L}, & \text{low irradiation level} \end{cases} \tag{12}$$

Unfortunately, some of the parameters required for numerical simulation are not usually available in the manufacturer's datasheets. For example, the series resistances R_s, the diode ideality constant n and the diode reverse saturation current I_s in Eq. (1) are typically not provided by the PV panel manufacturer. Basically, the only information one can get from datasheets of PV panels are: the nominal open-circuit voltage ($V_{OC,STC}$), the nominal short-circuit current ($I_{SC,STC}$), the voltage at the MPP (V_{MP}), the current

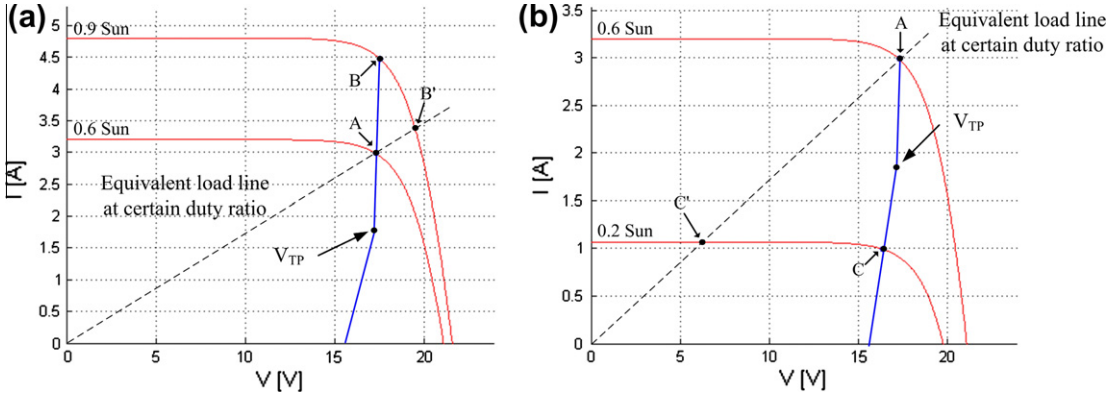

Fig. 5. The operating principle under a step change in irradiation level: (a) irradiation level increased from 600 W/m^2 to 900 W/m^2; (b) irradiation level decreased from 600 W/m^2 to 200 W/m^2.

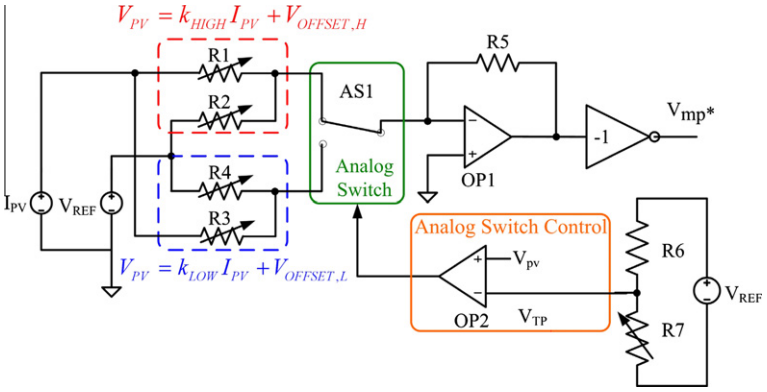

Fig. 7. Detailed implementation of the proposed analog MPPT.

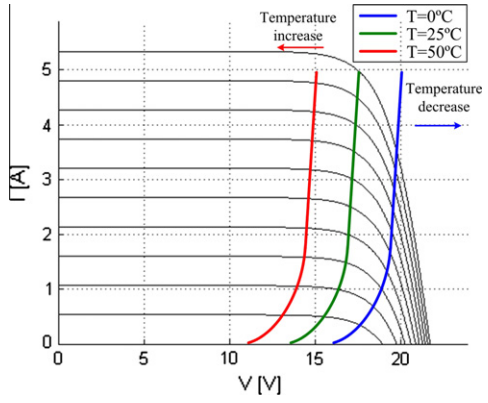

Fig. 8. The MPP locus for different operating temperatures.

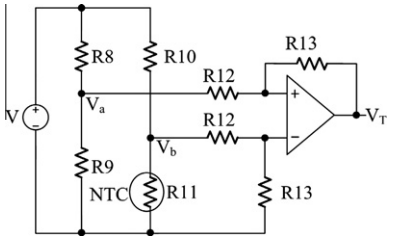

Fig. 9. Detailed implementation of the temperature compensation circuit.

Table 1
Parameters of the utilized PV panel.

Designation	KC85T
Maximum power (P_{max})	87.3 W
Open circuit voltage (V_{oc})	21.7 V
Maximum power voltage (V_{mp})	17.4 V
Short circuit current (I_{sc})	5.34 A
Maximum power current (I_{mp})	5.02 A
Temperature coefficient (α_v)	−0.082 V/°C

Table 2
Parameters of the implemented buck converter.

Component	Type
C_i	470 μF
C_o	470 μF
L_f	300 μH
Power switch	IRF540 N
Diode	STP10150

at the MPP (I_{MP}), the open-circuit voltage/temperature coefficient (K_V), the short-circuit current/temperature coefficient (K_I), and the maximum experimental peak output power ($P_{max,e}$). Therefore, an effective method which can be used to obtain the parameters of the I–V equation from practical data obtained in datasheets is required. In this paper, the technique proposed in Villalva et al. (2009) is utilized. This method is somewhat complicated because it uses iterative approach to obtain the solution. Therefore, to assist the system designer, a MATLAB-based program which can be used to automatically calculate the parameters of the approximation lines is also developed by the authors. The developed program can be found at https://sites.google.com/site/d9707203/code.

Fig. 4 depicts the block diagram of the proposed system. From Fig. 4, the reference voltage command is calculated using Eq. (12), and is then fed into a commercially available PWM IC. As in other MPPT methods, in order to acquire correct samples, the time interval between successive samples has to be greater than the system's settling time. On the other hand, the operation along the calculated MPP locus is carried out by the analog control loop of the PWM IC for the presented technique. Thus, the tracking time of MPP can be greatly reduced using the proposed technique. Fig. 5 illustrates the operation condition before and immediately after a step change in irradiation level for two cases. In Fig. 5a, the irradiation level is increased from 600 W/m^2 to 900 W/m^2. In this case, since both irradiation levels are considered as high irradiation, the operating point will change from point A to point B (for the proposed MPPT method) or point B′ (for conventional hill climbing method). On the other hand, the irradiation level is decreased from 600 W/m^2 to 200 W/m^2 in Fig. 5b. In this case, the operating point will change from point A to point C (for the proposed MPPT method) or point C′ (for

conventional hill climbing method). From both figures, the new operating point obtained using the proposed method is much closer to the real MPP than that attained by the conventional MPPT techniques. Consequently, fast tracking of MPP can be achieved. In addition, once the equilibrium point is reached, a further increase/decrease of the current will be prevented by the analog control loop of the PWM IC. As a result, phenomena like oscillations around the MPP or control losses due to sudden illumination variations will not occur. Therefore, higher tracking efficiency can be achieved.

4. Design procedure of the proposed system

The block diagram illustrated in Fig. 4 has been implemented as shown in Fig. 6 where the complete converter and its control circuit are depicted in detail. From Fig. 6, the presented system consists of a PV panel, a DC/DC converter, a commercially available PWM IC, an analog MPPT circuit and a temperature compensation circuit. In this paper, the PV panel employed is a multi-crystalline solar cell KC85T, with a nominal open-circuit voltage of 21.7 V and a nominal voltage value at the maximum power point of 17.4 V. For power stage, most of the MPPT systems proposed in the literature employ standard PWM-driven switch-mode power supply (SMPS) technologies. In this paper, a simple buck converter is used to interface the voltage from the PV panel to the load, and the PWM IC used is TL494 from Texas Instrument Corp. The implementation of this part of circuit is conventional, therefore will not be discussed further here.

The analog MPPT circuit shown in Fig. 6 can be realized using low power operational amplifiers (OPAMP) and an analog switch. From Eq. (12), two approximation lines should be implemented. Fig. 7 shows the detailed implementation of the analog MPPT circuit. In Fig. 7, two sets of resistors (R1–R4) and one OPAMP OP1 form an inverting summing amplifier with adjustable gain. The resistor values can be calculated as:

$$\begin{cases} \frac{R5}{R1} = k_{HIGH}, & V_{REF} \times \frac{R5}{R2} = V_{OFFSET,H} \\ \frac{R5}{R3} = k_{LOW}, & V_{REF} \times \frac{R5}{R4} = V_{OFFSET,L} \end{cases} \tag{13}$$

In Eq. (13), the voltage V_{REF} is a constant voltage and can typically be implemented by reference voltage available from PWM ICs.

From Fig. 5, the high irradiation line should be employed when PV panel voltage is greater than the turning point voltage V_{TP}, otherwise the low irradiation line should be used. To select the correct approximation line, a comparator OP2 and an analog switch AS1 is utilized, as shown in Fig. 7.

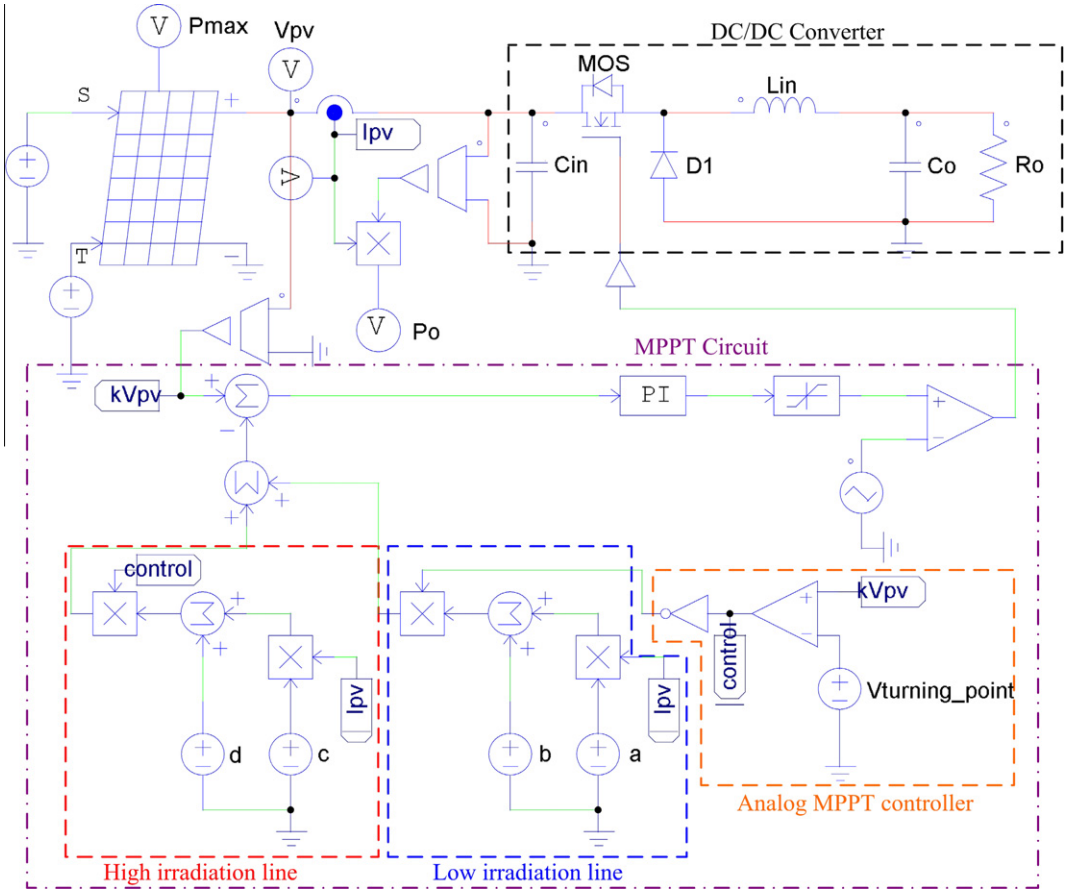

Fig. 10. Simulation model of the proposed system.

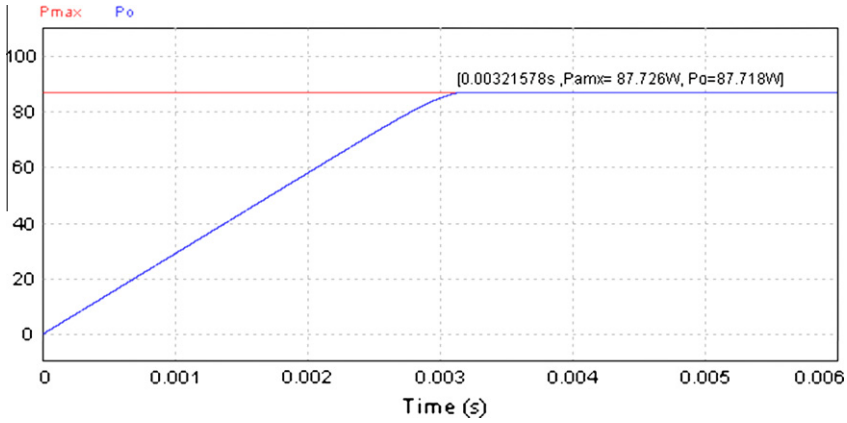

Fig. 11. Simulated starting waveform of the proposed system under standard test condition.

Fig. 8 shows the MPP locus for different operating temperatures. From Fig. 8, the MPP locus will shift right/left if the operating temperature decreases/increases. Therefore, an additional temperature compensation voltage V_T which is proportional to the panel temperature should be added to the voltage command V_{MP}^*. This concept can be implemented using the circuit depicted in Fig. 9. In Fig. 9, the voltage V_T can be expressed as

$$V_T = (V_a - V_b) \times \frac{R13}{R12} \tag{14}$$

where $V_a = V_{REF} \cdot (R9/(R8 + R9))$ is a constant voltage. When panel temperature increases, the resistance $R11$ will decrease and V_b will reduce, resulting in a higher compensation voltage V_T. The resistor ratio $R13/R12$ controls the offset quantity of V_T, which can be determined by the temperature coefficient α_V provided by the manufacturer.

From Fig. 6, the proposed MPPT method determines a reference voltage command V_{MP}^* corresponding to an atmospheric condition using PV panel voltage and current as inputs. Then, the PV panel voltage is sensed and compared with the command voltage V_{MP}^*. Through the PWM IC, an appropriate control signal is generated to regulate the PV panel voltage following V_{MP}^*, so that the DC/DC converter draws maximum power. Since the design procedures need not take the types of SMPS and PWM ICs into account, the proposed MPPT method can be applied to all types of SMPS using different types (for example, voltage mode and current mode) of PWM ICs.

5. Simulation and experimental results

To verify the correctness of the proposed analog MPPT method, an 87 W prototyping circuit is implemented from which simulations and experiments are carried out accordingly. The parameters of the utilized PV panel and the implemented buck converter are listed in Tables 1 and 2. Fig. 10 shows the simulation model of the proposed system.

In this paper, the simulations are made using PSIM 9.0. In PSIM 9.0, the PV panel can be implemented using the physical model of the solar cell in the renewable energy package. Fig. 11 shows the start waveform of the proposed system for standard test conditions (STC) of 1000 W/m^2 solar irradiance and 25 °C PV panel temperature. From Fig. 11, the proposed system can reach the MPP in less than 0.0033 s. It can also be observed that the oscillation around the MPP is very small thus can be neglected. The simulated results of the proposed system under different irradiation conditions are listed in Table 3, in Table 3, the tracking efficiency η is defined as

$$\eta = \frac{P_O}{P_{MAX}} \times 100\% \tag{15}$$

where P_O is the averaged output power obtained under steady state and P_{MAX} is the maximum available power of the PV panel under certain irradiation conditions. From Table 3, the tracking efficiency of the proposed system is higher than 99.22% for all irradiation levels.

Table 3
Tracking efficiency of the proposed system under different irradiation conditions.

S (W/m^2)	P_{MAX} (W)	P_O (W)	η (%)
100	7.779	7.747	99.60
150	11.99	11.91	99.39
200	16.29	16.16	99.22
250	20.75	20.66	99.58
300	25.21	25.16	99.81
350	29.45	29.41	99.88
400	33.86	33.84	99.95
450	38.41	38.39	99.95
500	42.77	42.76	99.98
550	47.23	47.21	99.97
600	51.75	51.74	99.98
650	56.22	56.20	99.97
700	60.75	60.73	99.97
750	65.26	65.23	99.95
800	69.61	69.58	99.95
850	74.12	74.06	99.92
900	78.51	78.44	99.91
950	82.96	82.85	99.87
1000	87.46	87.33	99.85

A prototyping circuit using the parameters shown in Tables 1 and 2 is also constructed. The proposed algorithm is validated using the Agilent Solar Array Simulator E4361 in SAS mode. For comparison, three other MPPT methods – the P&O method and the linear approximation methods proposed in Pan et al. (1999) and Scarpa et al. (2009) – are also implemented using the same hardware specification. Figs. 12 and 13 show the measured starting waveform for the commonly used P&O method and the proposed analog MPPT method, respectively. For the P&O method, the time step for one perturbation is set as 20 ms. From Figs. 12 and 13, the tracking times of the P&O and the proposed method are 1.02 s and 88 ms, respectively. In addition, the measured tracking efficiencies for P&O and the proposed method are 98.5% and 99.28%, respectively. It can be observed that apart from better overall power tracking with smaller oscillations in steady state, tracking with the proposed algorithm clearly displays faster dynamics. Fig. 14 shows the dynamic response of the proposed analog MPPT method under a step change in irradiation level. In Fig. 14a, the irradiation level is increased from 100 W/m^2 to 1000 W/m^2; in Fig. 14b, the irradiation level is decrease from 1000 W/m^2 to 100 W/m^2. In this paper, the turning point irradiation is set as 300 W/m^2. Therefore, 1000 W/m^2 can be regarded as high irradiation and 100 W/m^2 can

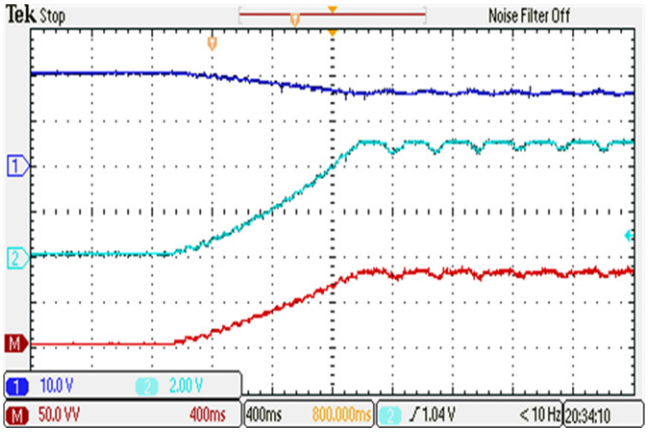

(CH1: V_{PV}, 10V/div, CH2: I_{PV}, 2A/div, MATH: P_{PV}, 50W/div, Time: 400 ms/div)

Fig. 12. Measured starting waveform for P&O method.

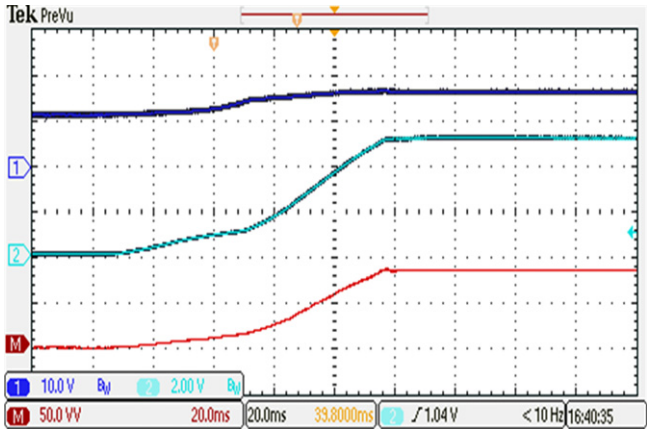

(CH1: V_{PV}, 10V/div, CH2: I_{PV}, 2A/div, MATH: P_{PV}, 50W/div, Time: 20 ms/div)

Fig. 13. Measured starting waveform for the proposed method.

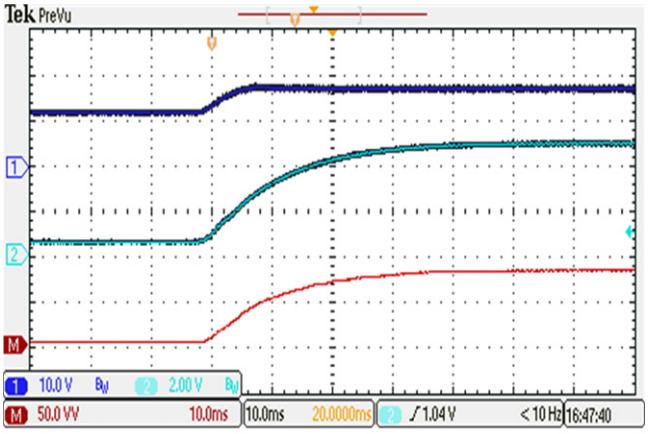

(a) Irradiation level increase

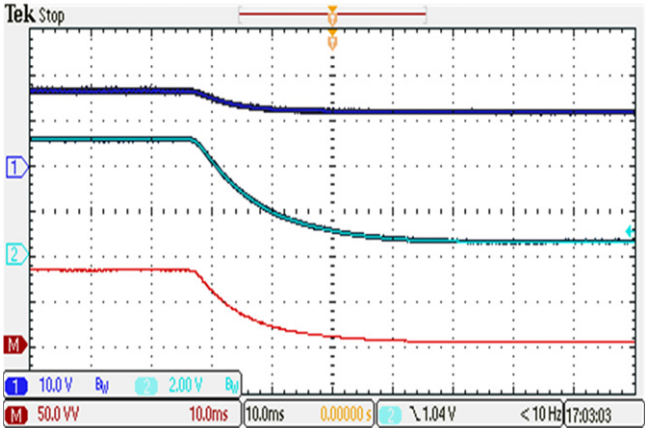

(b) Irradiation level decrease

(CH1: V_{PV}, 10V/div, CH2: I_{PV}, 2A/div, MATH: P_{PV}, 50W/div, Time: 10 ms/div)

Fig. 14. Measured starting waveform for the proposed method.

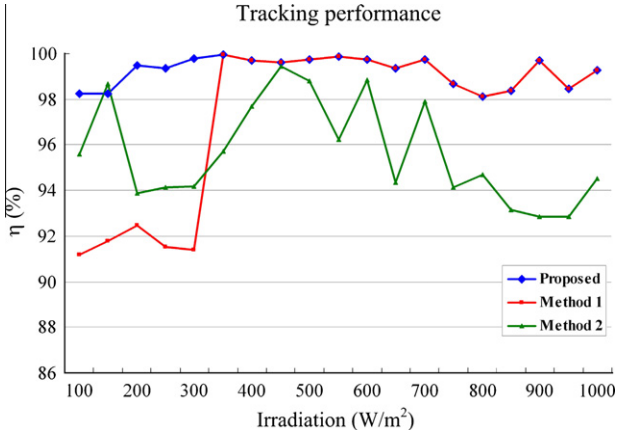

Fig. 15. Measured tracking efficiencies of three linear approximation methods.

Table 4
Summarized tracking efficiency data of three linear approximation methods.

Irradiation (W/m^2)	P_{MAX} (W)	Proposed method η (%)	Method 1 η (%)	Method 2 η (%)
100	7.779	98.26	91.20	95.57
150	11.99	98.22	91.78	98.67
200	16.28	99.46	92.48	93.87
250	20.63	99.34	91.53	94.15
300	25.01	99.80	91.40	94.18
350	29.42	99.94	99.94	95.70
400	33.85	99.69	99.69	97.69
450	38.30	99.59	99.59	99.43
500	42.76	99.75	99.75	98.80
550	47.22	99.88	99.88	96.23
600	51.69	99.72	99.72	98.85
650	56.16	99.35	99.35	94.37
700	60.63	99.74	99.74	97.90
750	65.10	98.69	98.69	94.12
800	69.57	98.09	98.09	94.69
850	74.03	98.37	98.37	93.13
900	78.49	99.69	99.69	92.86
950	82.94	98.44	98.44	92.83
1000	87.39	99.28	99.28	94.54

be regarded as low irradiation. From Fig. 14, the response times for increased and decreased irradiation level are 38 ms and 36 ms, respectively. Also from Fig. 14, the proposed method can move smoothly from high irradiation line to low irradiation line, and vise versa.

Fig. 15 illustrates the measured tracking efficiency for the proposed method and the methods presented in Scarpa et al. (2009) and Pan et al. (1999) (labeled as method 1 and method 2, respectively). These measured data is also summarized in Table 4. From Fig. 15, the tracking efficiencies of method 1 under low irradiation conditions is lower than the proposed method. This is mainly due to that the VAL of method 1 is calculated as the tangent line only for high irradiation conditions. Also observing Fig. 15, the tracking efficiencies of method 2 are all lower than those obtained by the proposed method. This is because only one VAL is utilized in method 2 to approximate all the points on MPP locus. From Table 4, the overall tracking efficiency of the proposed method is greater than 98.2% for both high and low irradiation conditions.

6. Conclusion

In this paper, a fast and low cost analog MPPT method for low power PV system is proposed. By using two VALs to approximate the MPP locus, high tracking efficiency can be achieved. Simulation and experimental results are also provided to demonstrate the effectiveness of the proposed technique. The main advantages of the proposed analog MPPT method are the following:

- It is very simple and can be implemented with low-cost, low-power analog components.
- The tracking speed is fast due to the utilization of analog control loop
- It does not require measurement of the PV power, that is, it does not require analog multiplier.
- It can be applied to all types of power converters.
- Its efficiency can be very high because, at steady-state, there are no oscillation around the MPP.
- It can easily be integrated into commercially available PWM ICs.

References

Ahmad, J., 2010. A fractional open circuit voltage based maximum power point tracker for photovoltaic arrays. IEEE International Conference on Software Technology and Engineering, 247–250.

Chu, C.C., Chen, C.L., 2009. Robust maximum power point tracking method for photovoltaic cells: A sliding mode control approach. Solar Energy 83, 1370–1378.

Chung, H.S.-H., Tse, K.K., Hui, S.Y.R., Mok, C.M., Ho, M.T., 2003. A novel maximum power point tracking technique for solar panels using a SEPIC or cuk converter. IEEE Transactions on Power Electronics 18, 717–724.

Dasgupta, N., Pandey, A., Mukerjee, A.K., 2008. Voltage-sensing-based photovoltaic MPPT with improved tracking and drift avoidance capabilities. Solar Energy Materials and Solar Cells 92, 1552–1558.

Dondi, D., Bertacchini, A., Brunelli, D., Larcher, L., Benini, L., 2008. Modeling and optimization of a solar energy harvester system for self-powered wireless sensor networks. IEEE Transactions on Industrial Electronics 55, 2759–2766.

Enrique, J.M., Andujar, J.M., Bohorquez, M.A., 2010. A reliable, fast and low cost maximum power point tracker for photovoltaic applications. Solar Energy 84, 79–89.

Esram, T., Kimball, J.W., Krein, P.T., Chapman, P.L., Midya, P., 2006. Dynamic maximum power point tracking of photovoltaic arrays using ripple correlation control. IEEE Transactions on Power Electronics 21, 1282–1291.

Esram, T., Chapman, P.L., 2007. Comparison of photovoltaic array maximum power point tracking techniques. IEEE Transactions on Energy Conversion 22, 439–449.

Femia, N., Petrone, G., Spagnuolo, G., Vitelli, M., 2003. A new analog MPPT technique: TEODI. Progress in Photovoltaic's: Research and Applications 11, 47–62.

Hohm, D.P., Ropp, M.E., 2003. Comparative study of maximum power point tracking algorithms. Progress in Photovoltaic's: Research and Applications 11, 47–62.

Hsieh, C.Y., Yang, C.Y., Feng, F.K., Chen, K.H., 2010. A photovoltaic system with an analog maximum power point tracking technique for 97.3% high effectiveness. Solid-State Circuits Conference, 230–233.

Kakosimos, P.E., Kladas, A.G., 2011. Implementation of photovoltaic array MPPT through fixed step predictive control technique. Renewable Energy 36, 2508–2514.

Kyocera Inc., 2007. Solar Cell KC85T. <http://global.kyocera.com>.

Leyva, R., Alonso, C., Queinnec, I., Cid-Pastor, A., Lagrange, D., Martinez-Salamero, L., 2006. MPPT of photovoltaic systems using extremum–seeking control. IEEE Transactions on Aerospace and Electronic Systems 42, 249–258.

Lopez-Lapena, O., Penella, M.T., Gasulla, M., 2010. A new MPPT method for low-power solar energy harvesting. IEEE Transactions on Industrial Electronics 57, 3129–3138.

Mattavelli, P., Saggini, S., Orietti, E., Spiazzi, G., 2010. A simple mixed-signal MPPT circuit for photovoltaic applications. Applied Power Electronics Conference, 953–960.

Messai, A., Mellit, A., Guessoum, A., Kalogirou, S.A., 2011. Maximum power point tracking using a GA optimized fuzzy logic controller and its FPGA implementation. Solar Energy 85, 265–277.

National Semiconductor Corp., 2011. Programmable Maximum Power Point Tracking Controller for Photovoltaic Solar Panels SM72442 Datasheet. <www.national.com>.

Pan, C.T., Chen, J.Y., Chu, C.P., Huang, Y.S., 1999. A fast maximum power point tracker for photovoltaic power systems. IEEE Industrial Electronics Conference, 390–393.

Park, J.H., Ahn, J.Y., Cho, B.H., Yu, G.J., 2006. Dual-module-based maximum power point tracking control of photovoltaic systems. IEEE Transactions on Industrial Electronics 53, 1036–1047.

Petreuş, D., Pătărău, T., Dărăban, S., Morel, C., Morley, B., 2011. A novel maximum power point tracker based on analog and digital control loops. Solar Energy 85, 588–600.

Salas, V., Olías, E., Barrado, A., Lázaro, A., 2006. Review of the maximum power point tracking algorithms for stand-alone photovoltaic systems. Solar Energy Materials and Solar Cells 90, 1555–1578.

Scarpa, V., Buso, S., Spiazzi, G., 2009. Low-complexity MPPT technique exploiting the PV module MPP locus characterization. IEEE Transactions on Industrial Electronics 56, 1531–1538.

Sokolov, M., Shmilovitz, D., 2008. A modified MPPT scheme for accelerated convergence. IEEE Transactions on Energy Conversion 23, 1105–1107.

STMicroelectronics Corp., 2011. High Efficiency Solar Battery Charger with Embedded MPPT SPV1040 Datasheet. <http://www.st.com>.

Texas Instrument Corp., 2009, Supplying TPS61200 With a Single Solar Cell. <http://www.ti.com>.

Texas Instrument Corp., 2011, Maximum Power Point Tracking Charger IC bq24650. <http://www.ti.com>.

Villalva, M.G., Gazoli, J.R., Filho, E.R., 2009. Comprehensive approach to modeling and simulation of photovoltaic arrays. IEEE Transactions on Power Electronics 24, 1198–1208.

Wang, J.C., Su, Y.L., Shieh, J.C., Jiang, J.A., 2011. High-accuracy maximum power point estimation for photovoltaic arrays. Solar Energy Materials and Solar Cells 95, 843–851.